Supplementary material

MATERIALS AND METHODS

1. Image pre-processing

We mapped land cover change in a study area (Landsat scene 15/053) over five dates: 1986/87, 1996/97, 2001, 2005, and 2011. Because of extensive cloudiness and Landsat 7 line errors, four of the five final images were mosaics of two to three image dates separated by less than thirteen months (see Table S1). We geometrically corrected each raw Landsat 5 image to Landsat 7 images to less than 0.5 RMS error using an automated tie-point program [1], then atmospherically corrected images using LEDAPS [2] and radiometrically corrected all images to the most haze-free image in the time series (November 15, 2011) using the MAD algorithm [3]. Prior to image mosaicking, clouds and line errors were masked using custom decision trees employing Band 1, 3, 4 and 6 thresholds, and water was masked using matched filtering followed by maximum likelihood classification to create thresholds for water omission. Next, we subset the image mosaics to center on the San Juan-La Selva Corridor and an adjacent 20 km buffer within Costa Rica, then masked areas above 500 m in elevation to omit deep topographic shading and coffee cultivation. The chosen 20 km buffer extended to the western edge of the selected Landsat image and delimited a region with similar geophysical characteristics and highway access; it excluded the eastern coastal wetlands and the seasonal rainfall regions closer to the Pacific.

Prior to classification, we selected six spectral bands (Landsat bands 1-5 and 7) and calculated four vegetation indices from the Landsat data. The vegetation indices were NDVI [4], the Brightness and Green bands from the Tasseled Cap transformation [5], and a normalized difference of Band 2 and Band 5 that distinguished banana cultivation (ND25, calculated like NDVI). These ten bands, along with elevation derived from a hole-filled SRTM DEM (v. 2.1) at 90 meter resolution [6,7], were the inputs into the classification.

2. Initial image classification: stable forest masks

In preliminary work, we could not readily distinguish secondary and primary forests in recent images; Landsat cannot accurately map tropical forest regrowth greater than 10-15 years in age [8,9]. As a consequence, we used the temporal information in our 25-year Landsat image time series to distinguish mature, stable forest from forest regrowth.

We began by classifying each image into forest and non-forest using a Random Forests classifier (n=1000 trees) [10]. Random Forests is an ensemble classification algorithm that creates a number of random decision trees and polls them for the modal prediction. It randomly selects a subset of predictors to split each decision tree node, and randomly withholds a subset of the training data at the start of the analysis for internal accuracy assessment ("out-of-bag", or OOB) [10]. We did not use the internal OOB accuracy from Random Forests, but instead withheld one third of the validation data prior to all classifications; Random Forests OOB accuracy was consistently higher than our independent validation data (data not shown) and all accuracy results here come from that validation data unless otherwise noted. All analyses were done using the randomForest package in R (v. 2.14.1).

Field data for land cover classification and validation consisted of GPS-located points from field campaigns in 2004-2005 and 2009-2011 [11]. Additional training and validation data came from high-resolution satellite imagery for 2011, high-resolution 2005 CARTA aerial photos [12], black-and-white aerial photos for 1986 and 1992, and geo-referenced forest and tree plantations boundaries from field surveys by a local forestry organization, FUNDECOR. Although it varied from year to year, the classifications used between 512 and 1082

polygons (covering 586-1223 ha each) for training data. As noted previously, more than one third of the training data were withheld for validation purposes prior to all classifications; this consisted of between 491 and 701 polygon centroids, depending on the year. For three years (1986, 2001, and 2011), we had sufficient data withheld to evaluate the change detection accuracy for forest-nonforest transitions.

The overall accuracy of each individual forest mask ranged between 94 and 96%. After classification, the forest/nonforest masks were integrated across time to separate each image into two areas: stable, unchanging forest, and areas that reforested, deforested, or remained open from the previous time period. In our longest time interval (1986 to 1996), it was possible for mature forest to directly transition to forest regrowth; this process occurs over a period of 5-7 years as forest is cut down and then rapidly regrows to a closed canopy. We explicitly assumed that images after 1996, which are 4-7 years apart, are sufficiently close together in time to map forest regrowth using forest masks.

For the 1996 image, following the modified methods of Helmer et al. (2009), we used the Random Forests classifier and our training data to distinguish light green regrowth areas from dark green mature forest; the internal OOB accuracy of this classification was 98.4%. To map young forest regrowth that occurred just prior to the time series, we then applied the1996-derived classifier to the 1986 image. After removing regrowth speckle smaller than 6 pixels (3x3 moving window sieve), we then removed all forest regrowth areas from the final stable forest masks for each year. Finally, although clouds obscured stable forests in some images, we assumed no change over time if the clouded areas remained forested in the ensuing time period. Any forest loss observed after clouds was assumed to occur in the time interval immediately preceding the cloud-free image.

3. Final image classification: all land cover classes

We performed two Random Forest (RF) classifications on each image; one for the stable forest area, and one for the change/open area. The 1986 map was predicted using the 2001 RF classifier; all other images were predicted by independent RF models. The stable forest area was classified into two possible land covers: mature lowland forest, and swamp forest, a distinct forest type on wet soils dominated by *Rafia taedigera* palms. "Mature" in this context denotes forest that is >25-30 years in age; all mature forests were stable forest on the 1986 image and had low spectral variability over time, implying an age of >30 years (see above).

The remaining change/open area was classified into ten land cover classes: four types of cropland (banana, pineapple, sugarcane, and palmito (heart-of-palm), pasture, bare earth, urban areas, and three types of forest cover (swamp forest, native reforestation, and exotic tree plantations). Native reforestation is defined as both native tree plantations and natural forest regeneration less than 25-30 years in age; native tree plantations in this region have a harvest rotation of 15-25 years and are often secondary forest species. Although natural forest regeneration is ecologically distinct from native tree plantations, high spectral overlap (producer's accuracies <70%) led to merging the two classes in the final classification. The exotic tree plantations were primarily teak (*Tectona grandis*, 15-20 year rotation) and gmelina (*Melina arborea*, 5-10 year rotation).

The resulting classified images were mosaicked together to create classified maps with twelve final land cover categories (Table S2). After classification, we applied a four-step post classification filter to reduce noise and eliminate spurious classification artefacts; these filters altered less than 16% of the classified pixels across all years (6-10% of pixels in a given year). Filtering the image to a 1 hectare MMU caused many of the pixel alterations. The first step consisted of the application of a majority filter using a 3x3 window to replace isolated small areas (<4 pixels) of swamp forest with mature forest. The second step applied two majority 3x3 moving window filters to remove speckle within the forest regrowth and nonforest areas, respectively. This step gave the final map a minimum mapping unit of approximately 1 hectare in size, without removing riparian forests surrounded by nonforest land covers.

The third step consisted of a series of temporal rules that corrected unlikely land cover transitions that often resulted from border misclassification or image mis-registration. Temporal rules included not allowing native regrowth to directly replace mature forest after 1996, or converting urban pixels that only occurred in one year ("temporal singlets") to bare earth: see Table S3 for a complete list. To correctly assign temporal singlets of cropland, we selected singlets with a low perimeter: area ratio (<20) to exclude agricultural fields and select edge errors. Then we used a moving 3x3 majority filter to replace the selected pixels with neighboring "green" land covers (cultivation, exotic tree plantations, or native reforestation). Where these edge singlets were bordered by bare earth and urban pixels, they were assigned to native reforestation.

Because temporal singlets in 2011 may be actual land cover change, we implemented fewer temporal rules in 2011. We allowed urban expansion within 1 km of previous urban areas and only replaced agricultural singlets that appeared completely within forest and were not connected to fields in open areas. Over the time series, almost all urban expansion occurred near towns and roads, and all agricultural expansion replaced open land at least in part.

In the fourth step, exotic plantations and crop fields smaller than 0.54 ha were assigned to other classes using a 3x3 filter (see Table S3); all exotic tree plantations the author observed were at least 1 ha in size, as were the vast majority of agricultural fields. In addition, narrow pineapple fields (perimeter:area ratio <20) were assumed to be edge errors and assigned to the bare dirt category to minimize misclassification of muddy riparian areas as pineapple. At the end of the temporal filtering, we filtered the image one last time to create a final1 hectare MMU; we used a minimum 10-pixel sieve followed by a 7 x7 majority filter on the sieved pixels.

4. Accuracy of final maps

The overall classification accuracy for the land cover maps ranged between 90 and 96%, depending on the year. The smallest omission and commission errors occurred for mature lowland forest, while the largest errors occurred in palmito (Table S4). Overall mission and commission errors were acceptable for native reforestation and exotic tree plantations, which were mainly confused with each other. Accuracies for cropland were lowest in 1986, when palmito was a large minority of all cropland, and improved dramatically in later years. Bare soil was least accurate in 2011, when it was frequently confused with pineapple fields under harvest.

To assess the change detection accuracy for forest-nonforest transitions, we took the final land cover maps and assigned classes to either forest (mature forest, swamp forest, exotic tree plantations, and native reforestation) or nonforest. Then we assessed change accuracy for a three-date combination where we had sufficient testing data over time for the eight possible land cover combinations (1986-2001-2011). Overall accuracy for the forest transitions was 93%; omission and commission errors were acceptable for all classes (Table S5). The least accurate class, Open-Open-Forest, was most commonly confused with Open-Forest-Forest, Forest-Open-Forest, and Open-Open-Open; this likely results from confusion between heavily wooded pastures and young secondary forests succeeding from wooded pastures. Combined producer's and user's accuracies for forest loss between 1986 and 2001 and forest loss between 2001 and 2011 were in excess of 88% (Table S5), although recent deforestation had poor accuracy before class combination (user's accuracy of 73%). Recent deforestation was confused with stable forest cover, implying that uncorrected, raw estimates of forest to nonforest transitions from 2001-2011 are underestimates of actual forest loss.

5. Estimation of land cover area changes

Using the land cover maps for each year, we extracted the land cover area and land cover transitions for the area of interest: the SJLS Biological Corridor and the adjacent 20-km buffers below 500 m (Figure S1a-e). We

corrected all raw land cover area estimates for differences in cloud and water areas among dates and then combined the eleven land cover classes into six classes for subsequent analysis (Table S2). We then compared the changes in land cover class area from 1986-1996 (pre-ban) to those from 1996-2011 (post-ban).

In a second analysis, we combined the above land-cover classes into two classes: forest and nonforest. We then corrected forest/nonforest class areas for differences in cloud areas among dates and then used the forest/nonforest classes to analyze forest loss in two different time periods (1986-2001 and 2001-2011) in a single, three-date change-detection accuracy analysis. We selected these two time periods because we had sufficient ground truth data in 2001 to assess change over time.

To correct the original area estimates of different land covers (derived from pixel counts) for classification error bias, we used the method described in Olofsson et al. [13]. We corrected area estimates for land cover classes and forest/nonforest cover using an error-adjusted stratified estimator. We then derived 95% confidence intervals around land-cover area estimates for each individual date; significant changes over time in area within a land cover class were inferred when confidence intervals of the different dates did not overlap [13].

Rates of annual loss and gain of land cover classes were calculated using the method of Puyravaud [14]; results for mature forest loss were robust to the rate method used (*data not shown*). To test whether the annual rate of mature forest loss differed over time, we used standard error propagation techniques to calculate a pooled standard error for mature forest cover on two dates [15], calculated a confidence interval for the difference in mature forest cover between the two dates (e.g., 1986-1996 or 1996-2011), and then divided by the time difference between the images to derive an upper and lower 95% confidence interval for the rate of mature forest loss. Calculation of the rate of total forest loss was simpler; we simply calculated the bias-corrected area and confidence intervals of the forest change classes for each date (from the stratified area estimator; see above) and then divided by the time difference between two dates to arrive at the rate of change and its 95% confidence interval.

6. Estimation of land-cover transitions

All land cover transitions in this paper, including transitions between forest and agricultural classes, were calculated with raw pairwise pixel transition data and then scaled to the corrected area estimate (see above) for a given source or destination class. Raw pairwise pixel transition data was gathered by comparing image-to-image pixel transitions across successive image-date pairs (e.g., 1986 & 1996) within the region of interest. All data were analyzed in summed transition tables and corrected for combined cloud area in both years; transitions to and from water were rare and ignored in the final analysis.

Ages and loss rates of native reforestation in our region were estimated using information from the classified land cover image dates. All native reforestation pixels that appeared for the first time in an image were conservatively assumed to at most two years of age; subsequent ages of native reforestation pixels were derived by tracking the persistence or disappearance of reforestation in the land cover map over time. Masked pixels were conservatively assumed to be reforested in previous and subsequent years, lowering the probability of observing transitions. Total native reforestation observed in each year was corrected to the corrected area estimates for that year (see above); the two totals were consistent. The oldest native reforestation was established in at least 1984 (two years prior to our oldest image) and inspection of aerial imagery for 1986 and 1992 revealed that tree plantations were quite rare in this time period. Thus, we can assume that the oldest age classes are primarily natural regeneration, not a mix of native tree plantations and naturally regenerating forests. The estimated area of secondary forest older than >20 years is less than 2% of mature forest area and has a small (<0.04%) effect on the calculated loss rate of legal forest in this paper. Similarly, native tree plantations typically have a harvest rotation

of 15-25 years, so we can also assume the majority of native reforestation converted to other land-uses at <10 years in age was converted natural regeneration, not tree plantations (Figure S5).

7. Calculating soil suitability of different land-uses

The agricultural capacity index map produced by the Costa Rican government [16] takes into account topography, drainage, soil fertility, and other factors to categorize the country into nine production zones, proceeding from land suited for crop production without limits to land only suited for protected forest cover. Our region did not include category I agricultural land, but only category II-IV (agricultural land with minor to heavy limits). We combined the production category map and the 2011 land cover map to estimate the area of selected land covers in different agricultural capacity rankings, and then normalized the results by the total land area in each agricultural capacity class (Figure S6).

[1] Kennedy R E and Cohen W B 2003 Automated designation of tie-points for image-to-image coregistration *International Journal of Remote Sensing* **24** 3467–90

[2] Masek J G, Huang C, Wolfe R, Cohen W, Hall F, Kutler J and Nelson P 2008 North American forest disturbance mapped from a decadal Landsat record *Remote Sensing of Environment* **112** 2914–26

[3] Canty M J and Nielsen A A 2008 Automatic radiometric normalization of multitemporal satellite imagery with the iteratively re-weighted MAD transformation *Remote Sensing of Environment* **112** 1025–36

[4] Tucker C J 1979 Red and photographic infrared linear combinations for monitoring vegetation *Remote sensing of Environment* **8** 127–50

[5] Crist E P and Cicone R C 1984 A physically-based transformation of Thematic Mapper data---The TM Tasseled Cap *Geoscience and Remote Sensing, IEEE Transactions on* 256–63

[6] Farr T G, Rosen P A, Caro E, Crippen R, Duren R, Hensley S, Kobrick M, Paller M, Rodriguez E, Roth L, Seal D, Shaffer S, Shimada J, Umland J, Werner M, Oskin M, Burbank D and Alsdorf D 2007 The Shuttle Radar Topography Mission *Reviews of Geophysics* **45** n/a–n/a

[7] Jarvis A, Reuter H I, Nelson A and Guevara E 2008 Hole-filled SRTM for the globe Version 4, available from the CGIAR-CSI SRTM 90m Database.

[8] Steininger M K 1996 Tropical secondary forest regrowth in the Amazon: Age, area and change estimation with Thematic Mapper data *International Journal of Remote Sensing* **17** 9–27

[9] Fagan M E and DeFries R S 2009 *Measurement and Monitoring of the World's Forests: A Review and Summary of Technical Capability, 2009-2015.* (Washington, D.C.: Resources for the Future (RFF))

[10] Breiman L 2001 Random Forests *Machine Learning* **45** 5–32

[11] Morse W C, Schedlbauer J L, Sesnie S E, Finegan B, Harvey C A, Hollenhorst S J, Kavanagh K L, Stoian D and Wulfhorst J D 2009 Consequences of Environmental Service Payments for Forest Retention and Recruitment in a Costa Rican Biological Corridor *Ecology and Society* **14**

[12] NASA 2005 *CARTA 2005 Final Flight Summary Report* (Moffett Field, California: SUBORBITAL SCIENCE PROGRAM, Airborne Sensor Facility, NASA Ames Research Center)

[13] Olofsson P, Foody G M, Stehman S V. and Woodcock C E 2013 Making better use of accuracy data in land change studies: Estimating accuracy and area and quantifying uncertainty using stratified estimation *Remote Sensing of Environment* **129** 122–31

[14] Puyravaud J-P 2003 Standardizing the calculation of the annual rate of deforestation *Forest Ecology and Management* **177** 593–6

[15] Moore D S 2004 *The basic practice of statistics* (New York: W.H. Freeman and Co.)

[16] MAG-MINIREM 1995 *La Capacidad de Uso de Las Tierras de Costa Rica* (San Jose, Costa Rica)

Table S1: Landsat image information

Year	Dates used	Type	Final masked area (%)*
1986/87	2/6/1986	Landsat 5	4.8
	3/13/1987	Landsat 5	--
1996/97	11/16/1996	Landsat 5	6.7
	12/21/1997	Landsat 5	--
2001	1/4/2001	Landsat 5	2.0
2005	2/2/2005	Landsat 7	33.5
	9/30/2005	Landsat 7	--
2011	11/15/2010	Landsat 7	7.6
	3/27/2011	Landsat 7	--
	1/15/2012	Landsat 7	--

***Cloud and line mask only**

Table S2: Mapped land cover classes

Summary class type	Classification class name	Short description
Cropland	Banana	Large, export-oriented monocultures of banana.
	Sugarcane	Large monocultures of sugarcane
	Palmito	Monocultures of heart-of-palm; in open or with shade trees
	Pineapple	Large, export-oriented monocultures of pineapple; often bare soil.
Other	Bare soil	Reddish exposed soil of region; mix of inceptisols and andisols.
	Urban	Mainly cement, asphault, and tin roofs; confused with river sand.
	Water	Open water, classified separately.
	Clouds	Masked prior to classification.
Pasture	Pasture	Open to wooded grassy pasture; dominant agricultural matrix.
Mature forest	Mature lowland forest	Forest >30 years old that is not palm forest. Majority is mature old-growth forest (see Supplementary text for details on age).
	Swamp forest	Forest >30 years old that is dominated by *Rafia* palms.
Forest regrowth	Native reforestation	Includes secondary regrowth forest and native tree plantations <30 years old. Native tree plantation spp. are common in 2° forest.
	Exotic tree plantations	Includes non-native plantations with *Teca* and *Gmelina* spp. only

Table S3: List of Temporal and Spatial Filtering Rules		
Order of Steps	Rule Description	Type of filter
1	Small swamp forest fragments (<0.36 ha) are unlikely; replaced by lowland forest.	Sieve 3x3
2	Two speckle filters for open and regrowth areas, respectively.	Majority 3x3
3	Transitions between swamp forest and lowland forest are unlikely; temporal majority is correct (lowland forest wins ties).	Temporal
4	Transitions between swamp forest and banana are unlikely (pasture intervenes); temporal majority of swamp forest replaces banana, and a banana majority replaces temporal "singlets" of swamp forest.	Temporal
5	By definition, mature lowland forest and swamp forest do not occur in time after open land covers; they are regrowth. This corrects edge and temporal filter errors.	Temporal
6	Temporal singlet urban pixels are unlikely since urban is a permanent land cover (except for 2011, where they may represent urban expansion). For 1986-2005, urban singlets are bare soil. For 2011, urban singlets are permitted only within 300 m of 2005 urban areas and otherwise are bare soil.	Temporal, spatial.
7	For 1986-2005, temporal singlet cultivation pixels (excluding bare soil transitions) that had low perimeter:area ratios (<=20) are green edge pixels. They are replaced by the majority of "bright green" neighboring pixels (see Supplementary text for description).	Temporal, Majority 3x3
8	For 2011, temporal singlet cultivation pixels that replace forest and do not touch adjacent open areas are ruled to be native reforestation.	Temporal, spatial.
9	Because direct transitions between exotic tree plantations and native reforestation are rare, we assigned confused pixels over time to the majority class (native regrowth wins ties).	Temporal
10	Because exotic tree plantations were unlikely to be less than 0.5 ha in size, small exotic tree plantations (<6 pixels in size) were sieved and ruled to be native reforestation.	Sieve 3x3
11	Because fields were unlikely to less than 0.5 ha in size, small cultivation fields (<6 pixels) were reassigned using a 3x3 majority filter to "bright green" neighboring classes. Fields surrounded by bare dirt or urban were left unchanged.	Majority 3x3
12	Repeat of Rule 3.	Temporal
13	Because of frequent spacing of satellite images after 1996, direct transitions between mature forest and regrowth are only allowed from 1986-1996; otherwise regrowth is replaced by mature forest.	Temporal
14	Narrow pineapple fields (perimeter: area ratio <20) were ruled to be edge errors and assigned to bare soil. Limited manual editing in 2011 to correct confusion of riverbeds with pineapple agriculture.	Spatial
15	Final 1 ha MMU filtering; sieved all clumps <10 pixels in size, then assigned sieved pixels using a majority filter.	Sieve 3x3, Majority 7x7

Table S4: Classification accuracy of individual image-dates

Classes	2011		2005		2001		1996		1986	
	Accuracy (%)		Accuracy (%)		Accuracy (%)		Accuracy (%)		Accuracy (%)	
	Prod.	User	Prod.	User	Prod.	User	Prod.	User	Prod.	User
Banana	87	98	98	100	100	98	98	98	70	88
Sugarcane	79	100	92	100	86	100	93	100	"	"
Palmito	71	79	80	94	67	83	"	"	"	"
Pineapple	98	95	96	100	92	100	100	100	"	"
Mature Forest	98	96	98	98	99	97	98	99	98	98
Native Reforestation	85	89	87	91	87	88	82	85	77	80
Exotic tree plant.	81	91	77	89	90	87	82	82	"	"
Pasture	95	83	97	86	93	87	100	91	96	91
Swamp forest	92	100	91	100	92	100	100	100	92	100
Urban	93	93	100	92	93	100	93	100	92	100
Bare soil	60	50	82	93	85	89	100	100	83	80
Overall	**90**		**93**		**93**		**96**		**93**	

Table S5: Classification accuracy of forest/nonforest change across three dates (1986-2001-2011)

Classes	Description		
		Accuracy (%)	
1986-2001-2011		Producer's	User's
Forest-Forest-Forest	Stable Forest	96	99
Open-Forest-Forest	Early persistent reforestation	92	93
Forest-Open-Forest	Deforestation then reforestation	92	75
Open-Open-Forest	Late reforestation	80	67
Forest-Forest-Open	Late deforestation	100	73
Open-Forest-Open	Reforestation then deforestation	90	95
Forest-Open-Open	Early deforestation	93	93
Open-Open-Open	Stable Nonforest	93	96
Overall		**93**	
1986-2001 deforestation	**F-O-O and F-O-F combined**	94	90
2001-2011 deforestation	**F-F-O and O-F-O combined**	92	88

Forest (F) and nonforest (O) transitions are from 1986 to 2001 to 2011.

Figure S1a-e: Classified land cover maps of northern Costa Rica. Clouds, cloud shadows, sensor line errors, and areas >500 m in elevation are masked in black. The following years are mapped: a) 1986, b) 1996, c) 2001, d) 2005, and e) 2011.

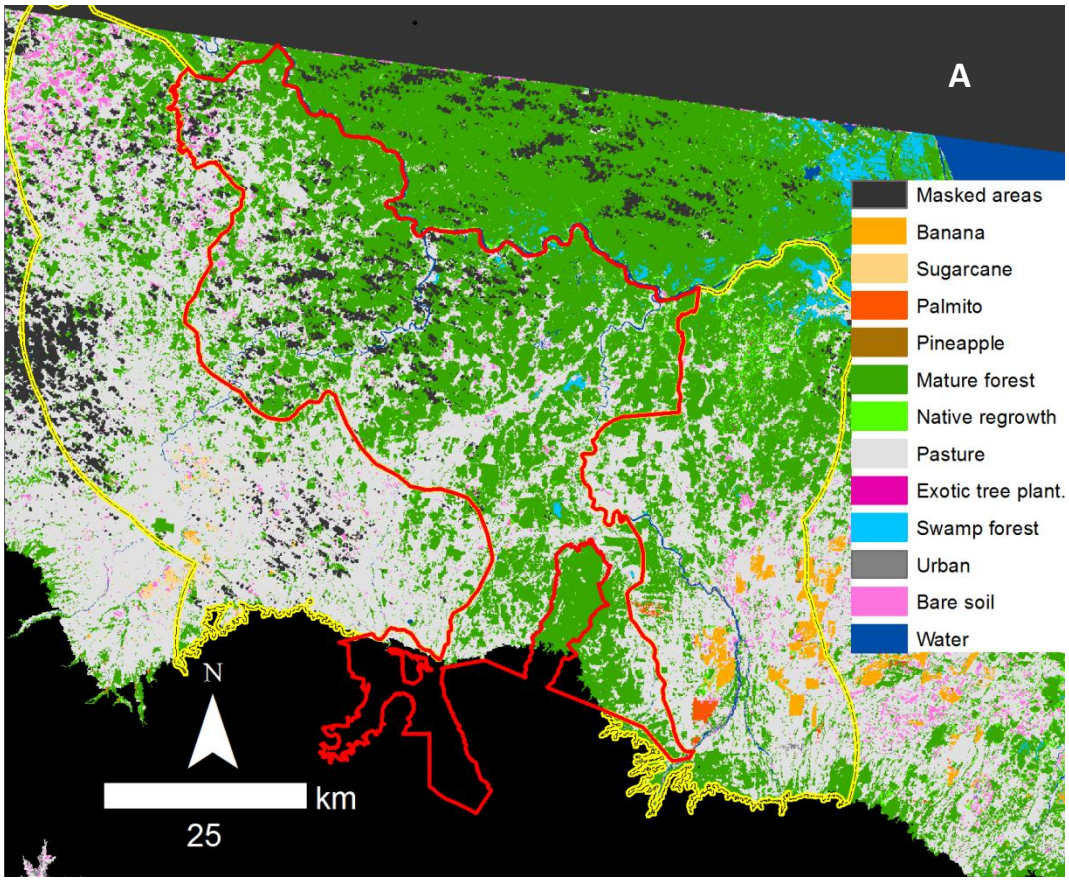

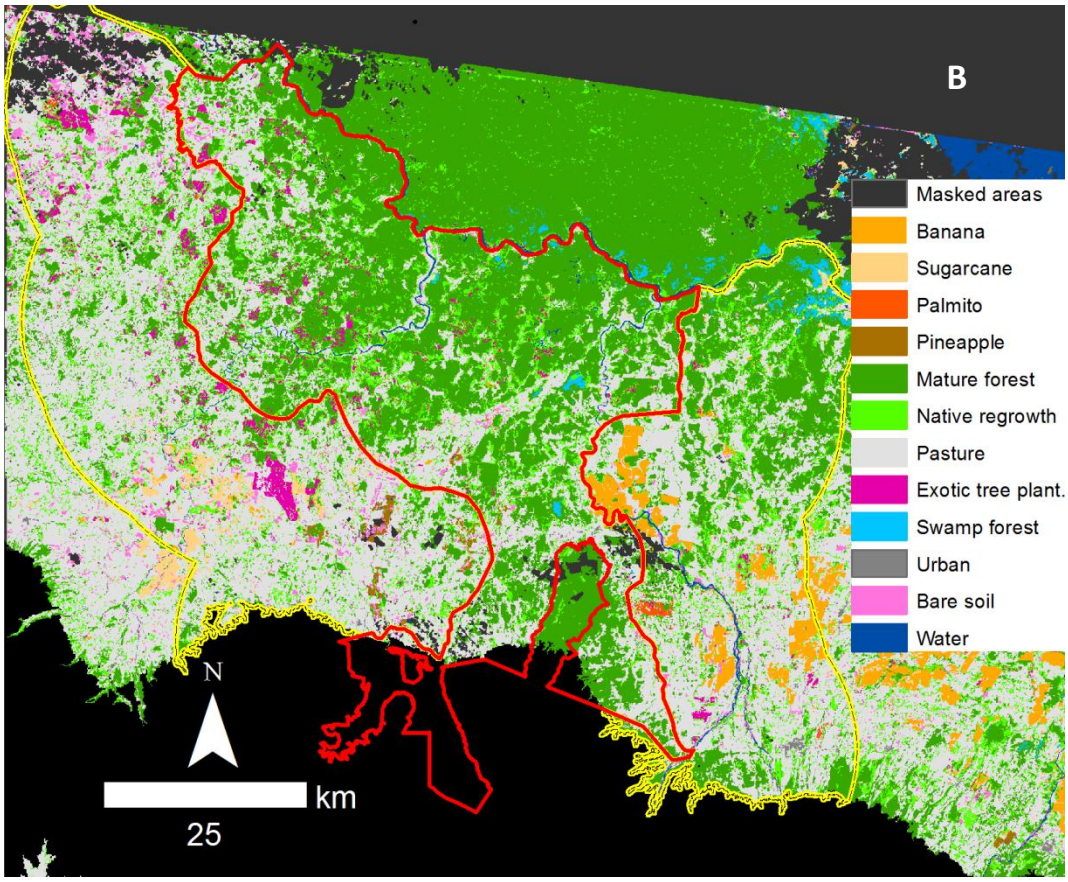

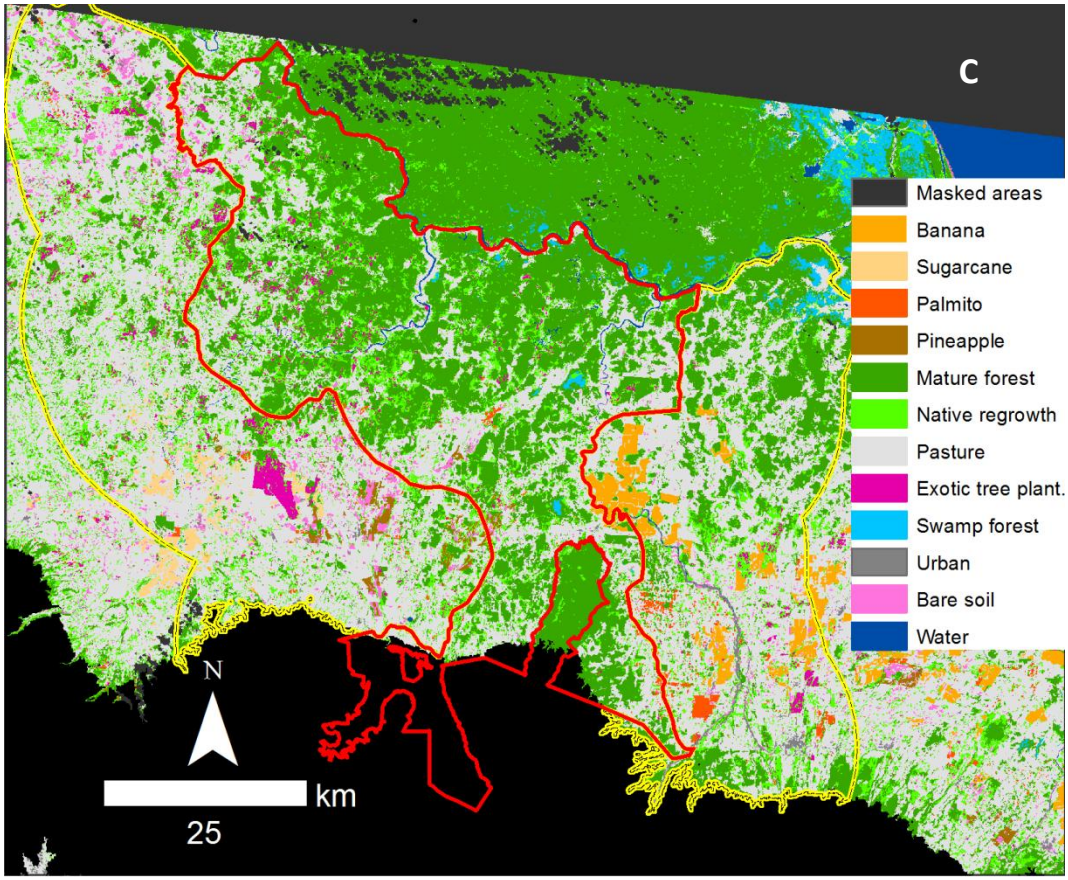

Fagan et al. 2013, ERL

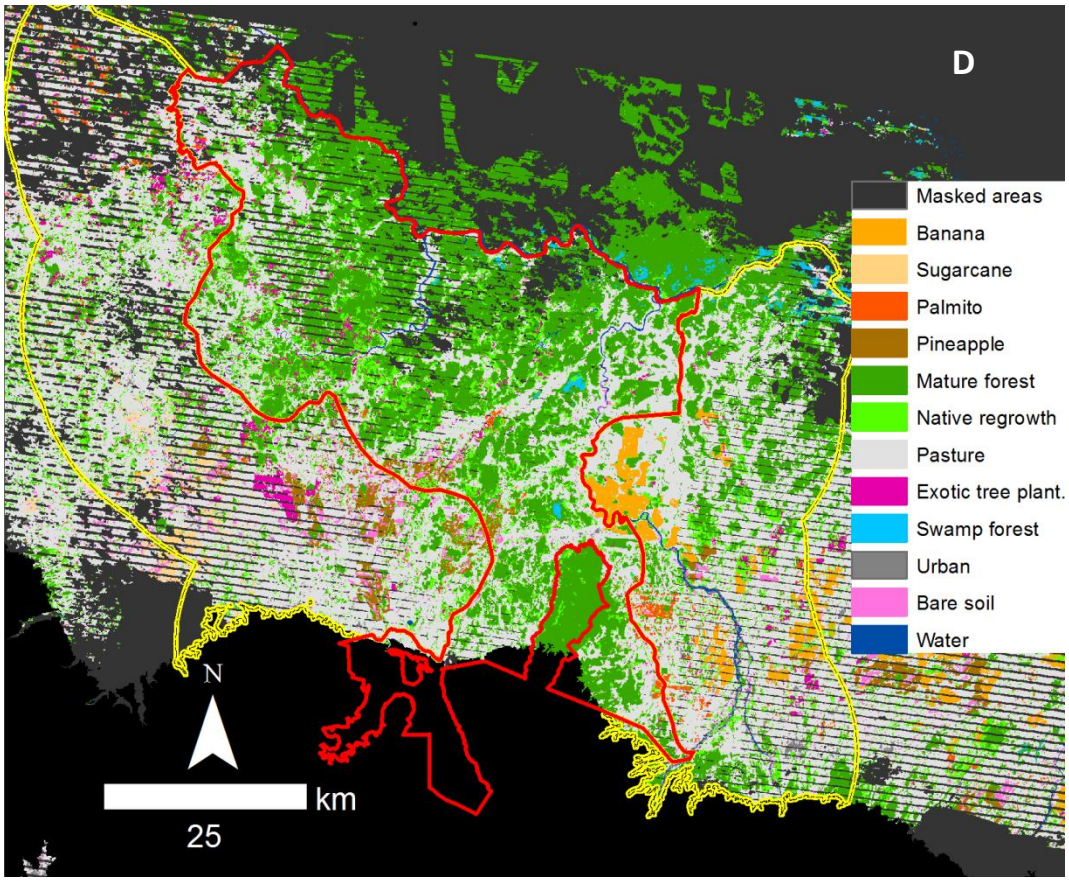

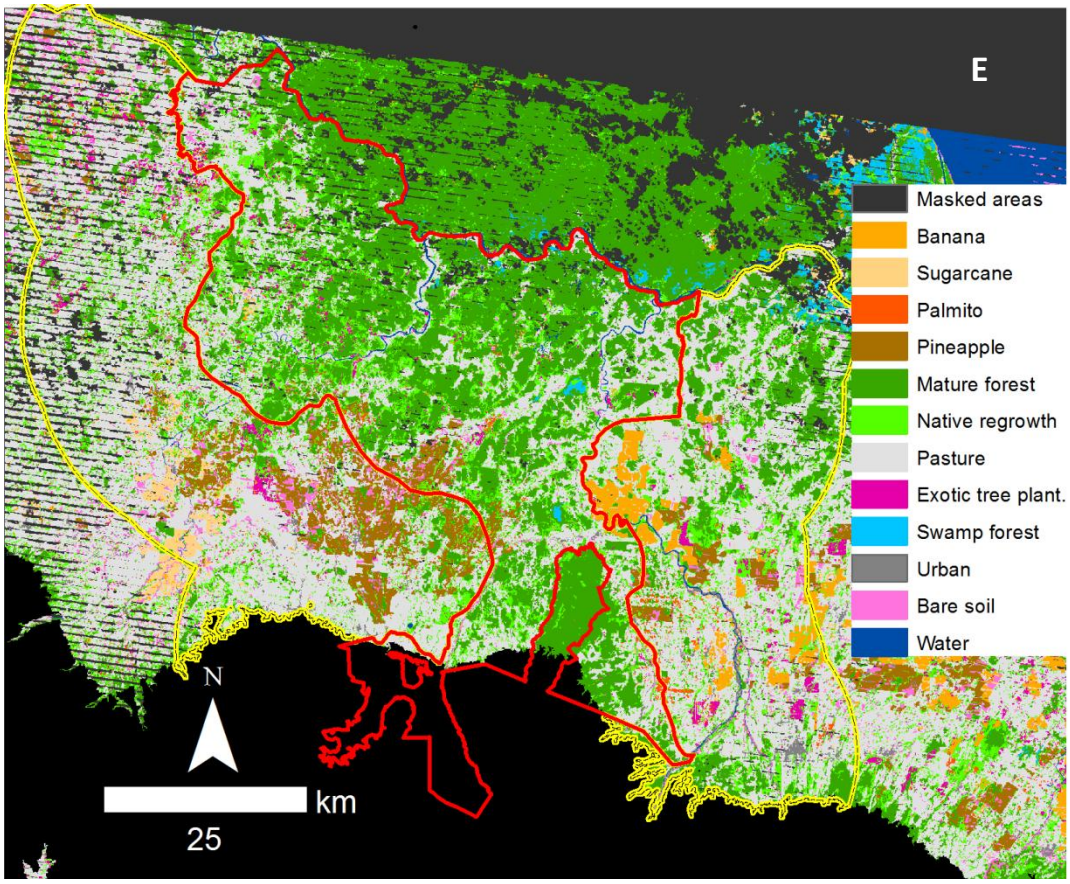

Fagan et al. 2013, ERL

Figure S2: Map of land cover changes over time in the region. We show deforestation and reforestation in two time intervals: 1986-1996 and 1996-2011. Native reforestation (NR) and exotic tree plantations (EP) regrew from 1986 to 1996, and may have persisted to 2011 or have been cleared between 1996 and 2011 (loss).

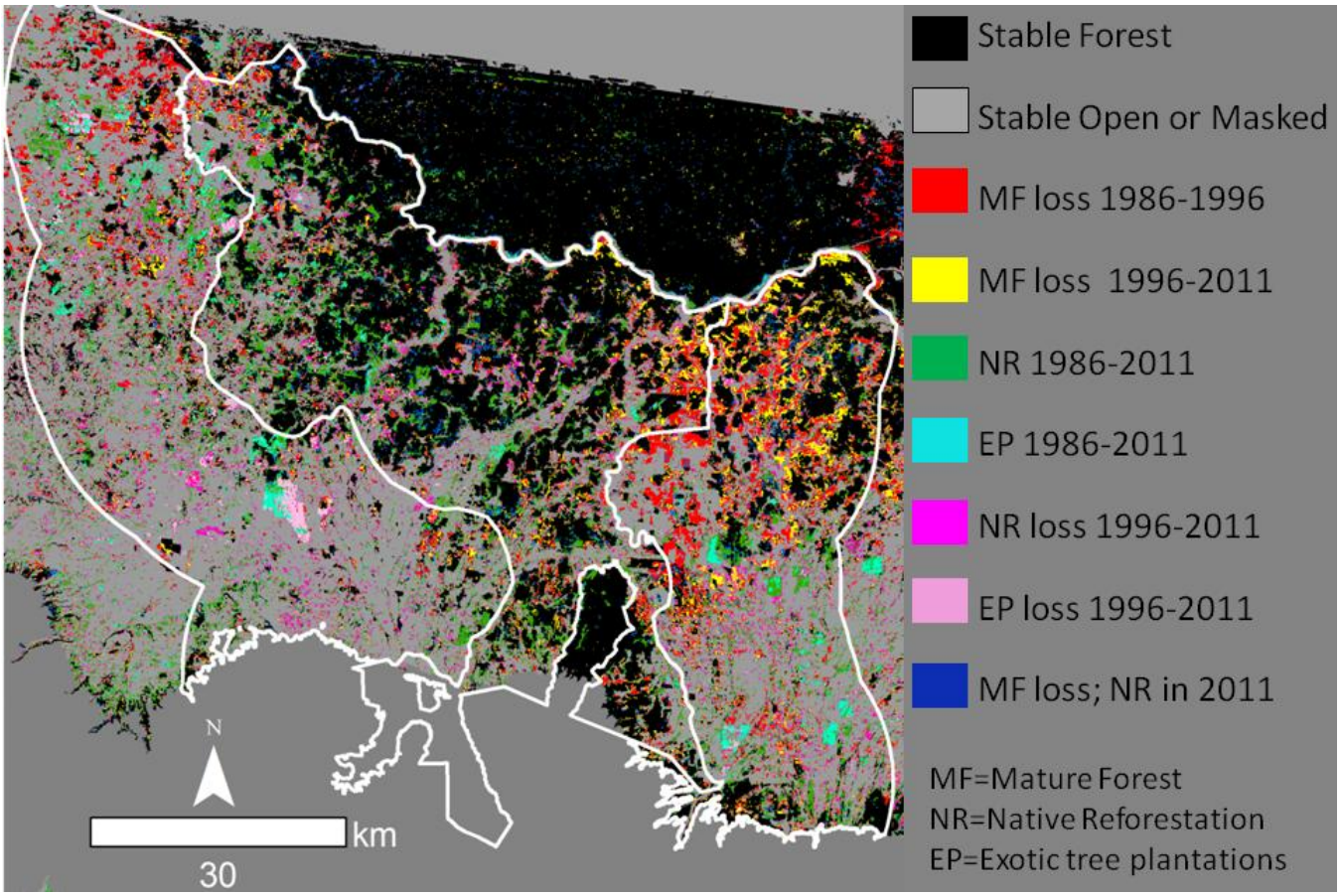

Fagan et al. 2013, ERL

Figure S3: Transitions of mature forest to other land-uses. The percentage of all deforestation to cropland is in yellow for each time interval.

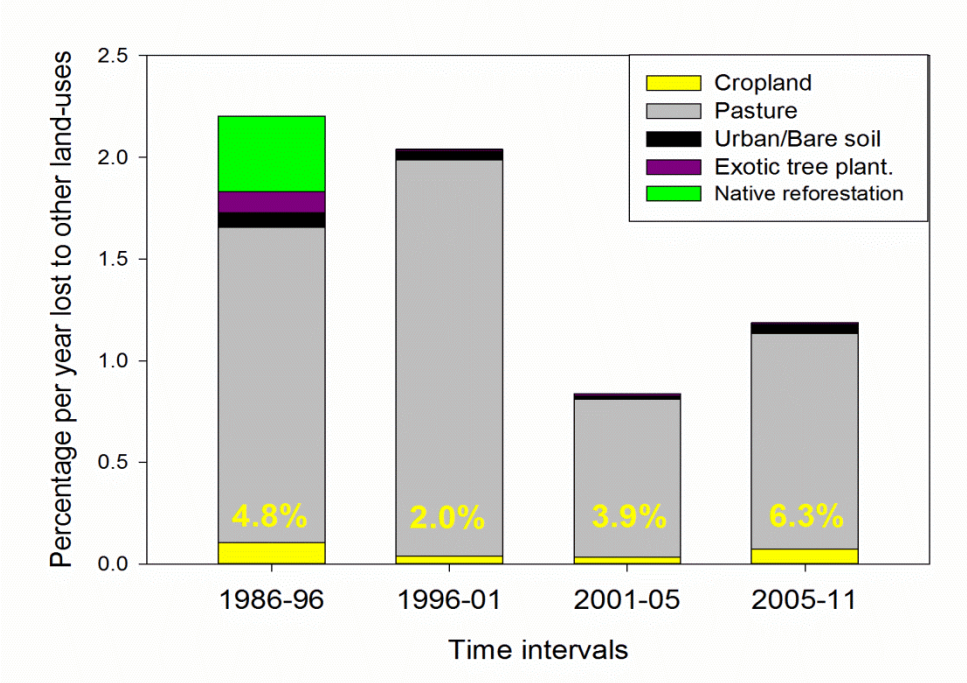

Figure S4: Graph of sources of native reforestation gain or loss. The top bars show the increase per year in new regrowth area; the bottom bars show loss of existing regrowth forest per year.

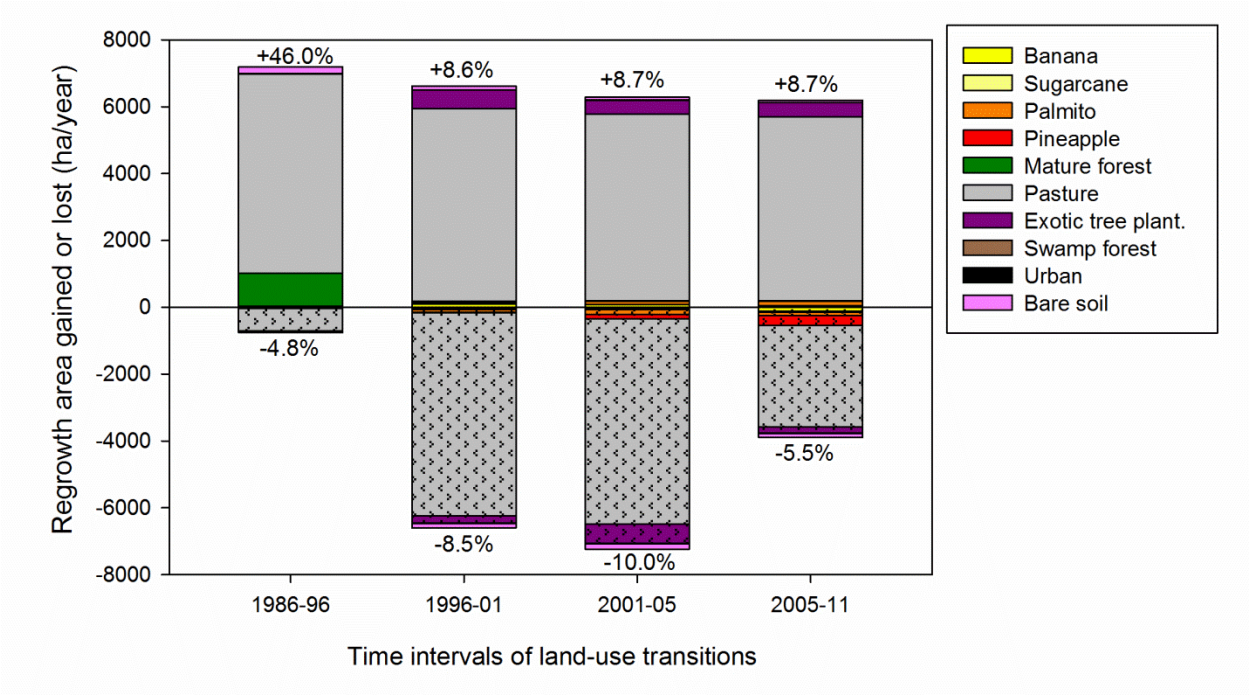

Fagan et al. 2013, ERL

Figure S5: Rates of loss of native reforestation, by age class. Note that native reforestation >21 years in age is assumed to be entirely natural regeneration based on aerial imagery.

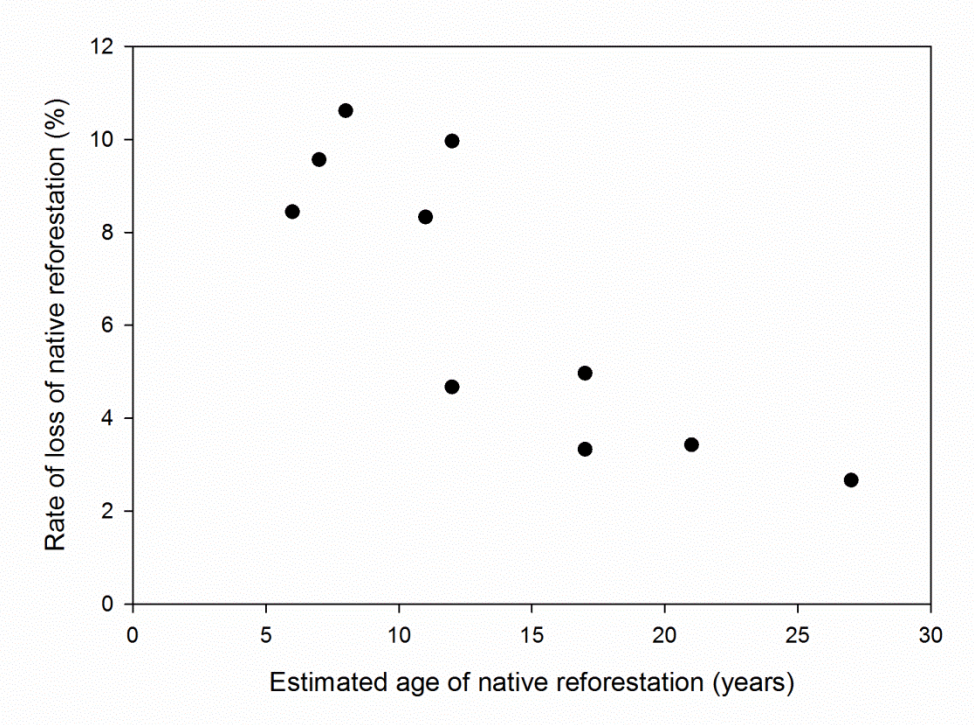

Figure S6: Comparisons of common land-use classes by agricultural capacity ranking, in 2011. Note that mature forest occupies substantial land under minor or medium limits for crop production, and pineapple is found across all index ranks. "Other non-crop" includes all agricultural capacity categories that deemed unsuitable for crop production; these include some protected areas that may contain suitable soils.

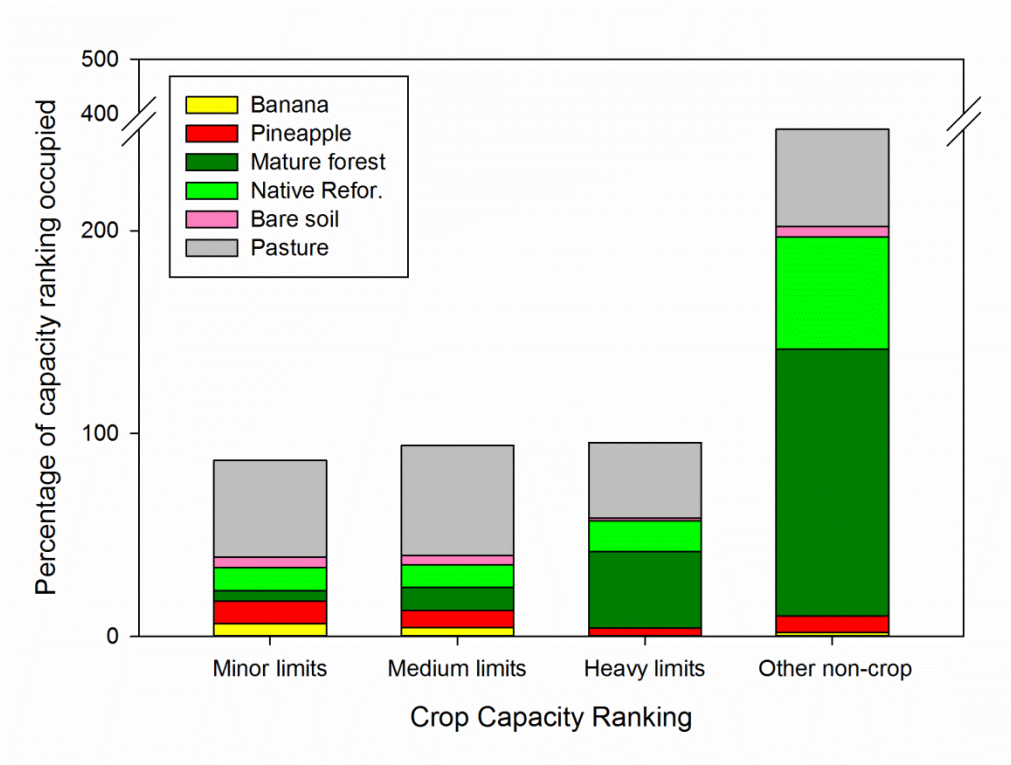

Figure S7: Expansion of different land covers over time. The mean annual area gained in three common land covers by expanding into other land cover classes. Pasture and pineapple expansion increased after 1996, while banana expansion briefly declined and then increased.